Comparative performance of terahertz emitters in amplifier-laser-based systems

Article *in* Semiconductor Science and Technology · June 2005

DOI: 10.1088/0268-1242/20/7/003

6 authors, including:

Markus Kress
Singulus Technologies S.A.
14 PUBLICATIONS **1,164** CITATIONS

Comparative performance of terahertz emitters in amplifier-laser-based systems

2005 Semicond. Sci. Technol. 20 S134

(http://iopscience.iop.org/0268-1242/20/7/003)

INSTITUTE OF PHYSICS PUBLISHING SEMICONDUCTOR SCIENCE AND TECHNOLOGY

Semicond. Sci. Technol. **20** (2005) S134–S141 doi:10.1088/0268-1242/20/7/003

Comparative performance of terahertz emitters in amplifier-laser-based systems

Torsten Löffler, Markus Kreß, Mark Thomson, Tobias Hahn, Noboru Hasegawa and Hartmut G Roskos

Physikalisches Institut, Johann Wolfgang Goethe-Universität, Max-von-Laue-Str 1, D-60438 Frankfurt (Main), Germany

E-mail: t.loeffler@physik.uni-frankfurt.de

Received 30 March 2005
Published 8 June 2005
Online at stacks.iop.org/SST/20/S134

Abstract

We give an overview of opto-electronic terahertz systems based on femtosecond amplifier lasers, and present a comparison of the relative performance and design issues of the various suitable downconversion photomixers employed for the generation of intense terahertz radiation pulses in such systems. The survey includes large-area biased semiconductor antennas, large-area nonlinear optical crystals and laser-generated gas plasmas as sources for terahertz radiation. The performance of these emitters is reviewed in terms of the terahertz pulse energies achieved and their associated spectral and signal-to-noise properties.

(Some figures in this article are in colour only in the electronic version)

1. Introduction

Pulsed opto-electronic terahertz (THz) techniques were first developed for systems employing high-repetition-rate (i.e. 100 MHz) femtosecond-pulse lasers [1–4]. However, soon after the technique was adapted to low-repetition-rate amplifier laser systems (with pulse energies typically in the μJ–mJ range) in order to gain access to higher THz-pulse energies.

The development for amplifier laser systems began with unbiased [5] and biased [6, 7] large-area semiconductor antennas. This type of emitter is discussed in section 4. In the following years, it was discovered that an increase of the THz bandwidth and improved beam quality could be achieved by photomixing in inorganic and organic nonlinear crystals [8–10]. This type of emitter is discussed in section 5. In addition, laser-generated plasmas have also emerged as powerful THz emitters [11–18] suitable for such high optical pump pulse energies. This type of emitter is discussed in section 6. A comparison of the relative performance of these various types of emitters is given in section 7.

2. Motivation for high-energy terahertz sources

Although amplifier lasers are relatively expensive and complicated to operate, there is a clear need for THz systems based on such lasers because of the comparatively high energy of the generated THz pulses, which can reach values of the order of 10 μJ with 1-kHz-repetition-rate systems and hundreds of μJ if 10 Hz systems are employed. Very high electric field amplitudes are associated with these high pulse energies. Upon tight focusing of the THz radiation, electric fields of tens of kV cm^{-1} for 1 kHz systems (or hundreds of kV cm^{-1} for 10 Hz systems) can be obtained, which is sufficient to access physical phenomena in a regime where they depend nonlinearly on the electric field (e.g. excitation of Rydberg states in atomic physics [19]). Moreover, amplifier lasers provide far higher signal strengths in optical-pump/THz-probe experiments. High-repetition-rate lasers are generally unsuitable for this purpose because the optical pump pulse energy is insufficient to provide the required excitation density over the full focal region of the THz probe beam, i.e., over a beam diameter of some hundreds of μm. An important example of such experiments is the measurement of transient photo-conductivity in optically-excited semiconductors [20].

In terms of applications, the development of amplifier-laser-based THz systems has been driven largely by the desire to develop single-shot electro-optic THz imaging systems [21]. The need for high THz-pulse energies in such systems stems from the fact that the dynamic range (in terms of detected THz spectral power) for each pixel decreases linearly with the number of pixels.

3. Motivation for large-area emitters

Before introducing the two main examples in sections 4 and 5 explicitly, we describe here some of the general properties of 'large-area' THz emitters (i.e. those with dimensions greatly exceeding the THz wavelength) in conjunction with amplifier laser THz systems.

Most THz emitters (excepting certain special cases such as plasma-based emitters, section 6) are effectively second-order nonlinear systems, i.e. the pulse-energy conversion efficiency over some area element of the emitter is linearly proportional to the incident fluence of the optical pump pulse [22]. In reality this only holds for an optical fluence which is low enough in order to avoid saturation (and optical damage thresholds). The ideal second-order nonlinear behaviour has two important consequences. Firstly, the THz-pulse energy scales with the square of the optical pulse energy. Secondly, for a constant optical pulse energy the THz-pulse energy is inversely proportional to the illuminated area of the emitter. This implies that the maximum THz-pulse energy following the emitter (for a given optical input pulse energy) will be achieved when the emitter area is reduced to an optimum value where a further increase in the ideal conversion efficiency from a smaller illuminated area is counteracted by the increase in saturation.

However, the situation changes if one aims at optimizing the peak THz-field amplitudes on the beam axis of a subsequent beam focus (e.g. at the THz detector). This quantity is actually more relevant to the performance of typical electro-optic detection schemes, where the optical probe beam is usually much smaller than the THz beam and effectively samples only the on-axis THz field. It can be shown from standard beam propagation theory (assuming a rational 'f_1 + f_2'-geometry in the placement of focusing elements throughout the THz imaging system [10]) that for a fixed THz-pulse energy and temporal waveform the maximum on-axis THz-field amplitude at a subsequent beam focus is proportional to the unfocused beam diameter at the emitter. Hence, assuming negligible saturation at the emitter this leads to the result that the detected THz-field strength will be independent of illuminated THz emitter dimensions (see [10] for details). Hence this allows one to overcome saturation effects whilst also achieving smaller diameter THz foci by increasing the illuminated emitter area (and the corresponding initial THz beam diameter) without a reduction of the electro-optically detected THz signal.

4. Large-area semiconductor antennas

The development of large-area antennas for use with amplifier laser systems began in 1990 [5] by employing semiconductor surface emitters, which had been previously developed for high-repetition rate systems [23]. Soon after it was established that externally-biased semiconductors (e.g. GaAs and InP) can achieve superior performance as THz emitters [6, 7, 24, 25].

The concept of this type of emitter is straightforward. A semiconductor wafer, with dimensions typically $\sim$3 cm $\times$ 3 cm, is biased with two electrodes to build up an electric field across the wafer of up to 15 kV cm^{-1}. In order to achieve such high bias field values one has to use a pulsed high voltage source delivering up to 45 kV with a pulse duration in the μs-range in order to avoid electrical breakdown. If an ultrashort optical pulse is incident on the wafer (after an appropriate expansion of the optical beam), carriers are generated and separated in the field. This leads to a transient surface current which generates the THz radiation. A comprehensive treatment of this process is given in [7]. The generation of THz-pulse energies up to 800 μJ with a biased GaAs antenna has been reported [6]. This corresponds to a energy conversion efficiency of the order of 10^{-3}.

Although these results are impressive, there are a few important drawbacks of such large-area pulse-biased antennas. One key practical issue concerns the use of a pulsed high-voltage source, which produces a large amount of ambient electromagnetic noise. This results in large amounts of noise interference with the detection electronics which degrades the dynamic range of the detected THz signal, unless considerable effort is employed to isolate different parts of the measurement system. From our experience, a preferable strategy is to employ more modest dc bias fields (of the order of 1 kV cm^{-1}), which produce far less transient electromagnetic noise. With such a system one can achieve THz-pulse energies of up to 1–2 μJ and conversion efficiencies in the range $\sim 10^{-6}$–10^{-5}. In the following sections we will regard statically-biased antenna emitters with these operation parameters as representing state-of-the-art performance for practicable THz systems.

A second limiting factor in the performance of biased antennas is the fact that the THz conversion efficiency (which ideally scales linearly with the laser pulse energy) starts to saturate at relatively low laser pulse fluences. The predominant mechanism for this saturation is the screening of the bias field by the local generated THz field [6, 7, 24, 25] (whilst an additional far weaker screening effect is introduced by the separation of the free carriers [26]). Such screening effects make it difficult to take advantage of laser pulse energies exceeding $\sim$100 μJ. The only way to overcome this situation would be to further increase the size of the emitter antenna (and the corresponding bias voltage), although this becomes unpractical when the size exceeds that of standard semiconductor wafers. We also note that the effect of strong saturation in combination with a residual initial carrier distribution and bias-field inhomogeneities leads to an asymmetric emission pattern for the THz beam which deviates strongly from a Gaussian form [27]. This leads to aberrations which are problematic for THz imaging systems [28] (especially for those employing dark-field techniques [29, 30]).

5. Large-area nonlinear crystal emitters

Large-area electro-optic crystals offer a promising alternative to large-area biased antennas as THz emitters for amplifier-laser-based systems. Although the conversion efficiency is significantly lower than that for biased GaAs antennas in the low-signal limit, the higher inherent saturation threshold of the THz generation process for nonlinear crystals results in a comparable or even superior performance for laser pulse energies of $\sim$500 μJ. The difference-frequency generation mechanism is usually referred to as 'optical rectification', and

has been extensively studied for THz systems employing low-pulse-energy, high-repetition-rate femtosecond lasers [2–4]. In these systems one usually works with tightly focused optical pump beams (typically with $\sim$10 μm diameter), although in the case of amplifier laser pump sources one generally must use unfocused beams in order to remain below the saturation and damage thresholds.

The most critical issue in electro-optic THz generation (and detection) applies to both low- and high-pulse-energy systems, i.e. to find suitable crystals with low optical- and THz-absorption in conjunction with favourable phase-matching between the THz phase- and optical-group velocities. If these conditions were to be perfectly fulfilled, the generated THz pulse energy should scale quadratically with the path length of the emitter crystal until saturation is reached.

The most common nonlinear crystal employed for Ti:Sapphire based lasers (which operate at around 800 nm) is ZnTe. This material possesses attractive phase-matching and THz transparency characteristics over a frequency range up to $\sim$3 THz [4] and possesses a high electro-optic coefficient. Such large-area emitters have already been used in several applications and in order to explore the potential of new organic electro-optic materials [8, 9]. However, there are not many contributions discussing the impact of the emitter size on the performance of THz systems. We, therefore, recently performed a detailed study on this type of emitter [10]. The results of a 2 mm thick 25 mm diameter ZnTe emitter are summarized in the comparative data in section 7.

6. Terahertz emission from laser-generated plasmas

A very different class of THz emitters which are suitable for use with amplifier laser systems is based on laser-generated plasmas. The basic concept of these emitters is to focus a short high-energy laser pulse in a gaseous medium (e.g. air). By doing so one reaches optical field strengths which are high enough to ionize the air and form a plasma in the focal region. If one now manages to achieve a net polarization within the plasma, the time-dependent macroscopic dipole-moment will lead to the emission of THz radiation. We will now discuss different methods that achieve such a net polarization within the plasma.

6.1. Emission based on ponderomotive forces

THz emission from a laser-pulse-induced plasma was first demonstrated by Hamster *et al* [11–13]. The mechanism leading to the net THz emission from the photoinduced plasma was attributed to the polarization produced by the free electrons that are accelerated by the ponderomotive forces associated with the propagating laser pulse, i.e. due to a spatio-temporal optical intensity gradient within the plasma. In these experiments, a rotationally symmetric polarization is created around the beam propagation axis. Hamster *et al* showed both numerically and experimentally that this leads to an emission of THz radiation in a diverging cone about the optical propagation axis. Due to symmetry reasons no net THz field radiates along the optical propagation axis. The energy of the THz pulses generated by this method is relatively low compared to alternative schemes employing laser-induced plasmas (see data in section 7). However, it is interesting to note the results of recent theoretical calculations, which indicate that THz emission based on this effect might be greatly enhanced if very short pulses in the 10 fs regime are used [31].

6.2. Emission based on external fields

One method to increase the THz radiation and to direct it into the forward direction is to apply an external bias field to the region where the plasma is formed and transverse to the optical propagation axis [16]. In this case, THz generation is associated with ultrafast screening of the external field within the plasma, and the corresponding displacement current is the source of an intense THz pulse. The resultant THz-pulse amplitude (energy) scales linearly (quadratically) with the external bias field, as is the case for most opto-electronic emitters. The maximum achievable THz-pulse energy for a given laser pulse energy is limited by the maximum external bias field which can be applied without dielectric breakdown of the gas. We have previously demonstrated that the breakdown field, and accordingly the maximal THz-pulse energy, can be enhanced significantly if the gas pressure is increased above atmospheric pressure [17].

6.3. Emission based on 'optical second harmonic bias'

Significantly higher THz-pulse energies which are comparable to those available from large-area emitters can be achieved if the laser pulse used to generate the plasma consists of both fundamental and second-harmonic (SH) spectral components, which creates an asymmetry in the optical electric field. Two different models have been put forward to discuss the mechanism responsible for the observed THz emission [32, 33], which we address in the following.

In initial reports, Cook and Hochstrasser attributed the THz generation process to four-wave rectification mediated by the third-order nonlinearity of air [14], but later noted that achieving photoinduced ionization (plasma formation) plays a role in the THz generation process [15]. In order to elucidate the mechanism for THz generation further, we extended the experiments of Cook and Hochstrasser, and found conclusive evidence that plasma generation is essential for significant THz emission from the focal region [18]. Accordingly, the four-wave-rectification picture introduced by Cook and Hochstrasser had to be modified in an appropriate way in order to account for the influence of the plasma volume.

One possibility is to maintain a description in terms of a four-wave rectification process, but with a finite nonlinear polarization only in the spatial region where significant ionization occurs [33]. But it should be noted that in order to be consistent with the experimental magnitude of the observed THz emission, such a model requires a relatively large value of the third-order nonlinear susceptibility of the plasma medium itself, although so far there is no experimental evidence to support such a large value [34].

Another way to explain the THz emission is that the spatio-temporal ionization process itself leads to an effective polarization within the plasma which is responsible for the THz emission [32, 33]. A detailed introduction of this model is beyond the scope of this paper and will be published elsewhere [35].

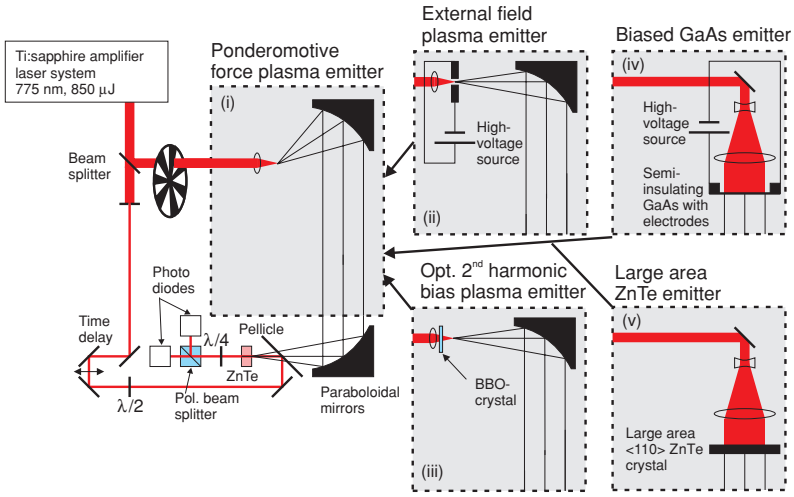

Figure 1. Experimental set-up for the various sources.

It should be noted that both models predict the experimentally-observed dependence of the amplitude and polarity of the emitted THz field on the relative phase and polarization between the fundamental and SH optical fields [14, 18]. Moreover, both models predict the observed super-quadratic increase of the THz-pulse energy (i.e. a super-linear growth of the THz electric field amplitude) with the laser pulse energy.

7. Experimental results and comparison

7.1. Experimental set up

In our experiments, we employ a 1 kHz Ti:sapphire laser system (Clark-MXR CPA-2001), which provides ∼150 fs laser pulses (intensity FWHM) at 775 nm with a maximum pulse energy of 860 μJ. A schematic of the generic THz system and the appropriate beam geometry for each THz emitter (labelled (i)–(v)) is shown in figure 1, and explained in the following. The use of standard off-axis paraboloidal mirrors for collimating and focusing the THz radiation and the details of the electro-optic detection (including the use of 500 Hz chopping of the optical pump beam and lock-in detection) have been described elsewhere (e.g. [33]). Note that all the plasma-emitter results presented here are for focusing in air at atmospheric pressure.

(i) For measurements of signals resulting from unbiased plasmas (i.e. due to ponderomotive forces), the fact that the maximum THz emission does not occur in forward direction must be considered. As shown, the emitted THz field is collected using an off-axis paraboloidal mirror with its effective optical axis displaced laterally with respect to the optical pump beam axis.

(ii) In measurements with electrically biased plasmas, two electrodes with round tips apply an external field to the region where the plasma is generated and the THz radiation emitted in forward direction is guided to the detector.

(iii) Following the SH-biasing approach of Cook and Hochstrasser [14, 15, 18], laser pulses are focused into a 100-μm-thick β-barium-borate (BBO) crystal which is cut so as to achieve type-I phase-matching for second-harmonic generation (SHG) of the 775 nm fundamental light. The SHG efficiency is controlled by varying the position of the BBO crystal with respect to the subsequent beam waist where the photoinduced plasma (and THz radiation) is generated. Because of the different phase velocities of the ω- and 2ω-fields in air, the relative phase between the fundamental and the SH components at the focus depends on the optical path length between BBO crystal and focus. The measurements described in the following are performed with the relative phase optimized for maximum THz-generation efficiency which is achieved by tilting a glass platelet in the beam path until maximum THz power is obtained.

(iv) A standard large-aperture GaAs emitter [6, 7, 24, 25] serves as a reference emitter. It consists of a semi-insulating GaAs wafer with metal electrodes defining an active emitter area of 3 cm × 3 cm. The optical pump beam is suitably expanded with the aid of a telescope arrangement as shown. The static bias employed here is 1 kV cm^{-1}.

(v) Here an unbiased ZnTe crystal is employed as the THz emitter based on optical rectification. The large-area ZnTe crystal used here has a diameter of 25 mm and a thickness of 2 mm, and is cut with a ⟨1 1 0⟩-orientation, which allows one to achieve the maximum nonlinear polarization available with a suitable azimuthal rotation of the crystal.

In the case of all three plasma sources ((i)–(iii)), the emitted THz radiation is collimated by an off-axis paraboloid (with an effective focal length of $f = 50$ mm) and then focused with a second one (also with $f = 50$ mm) onto a 1-mm-thick ZnTe crystal for electro-optical detection. In the case of the large-area emitters, the first paraboloid is excluded because the emitted THz beam from the large-area emitters is already optimally collimated.

7.2. Time and frequency domain data

Typical experimental THz time-domain signals for each emitter are shown in the right-hand panels of figure 2 (excluding the unbiased plasma).

In figure 2(a) the detected (on-axis) temporal THz electric field using the ZnTe emitter is shown, for the case of a pump beam diameter of 24 mm and an optical pump pulse energy of

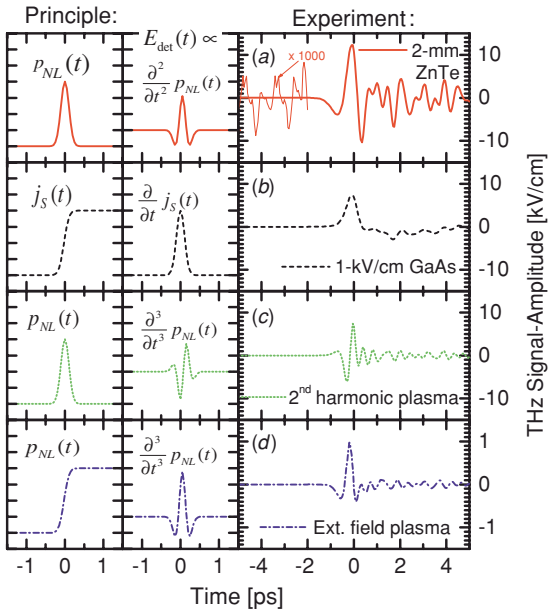

Figure 2. Right: experimentally obtained time domain data for the various sources. Left: illustrations for the origin of temporal signal forms.

360 μJ. These data were acquired using a single delay-stage scan with a lock-in time constant of 30 ms. The section of the graph from -5 to -2 ps is also shown enlarged by a factor of 1000. This expanded section of the THz trace indicates that the noise floor of the detection system before the main pulse (or, equivalently in this case, in the absence of a THz signal) is approximately 10 V cm^{-1}, which gives an indication for the smallest detectable THz field amplitude. Hence in terms of dark noise alone, the dynamic range of our system is of the order of 1000 for the detected THz electric field, or 10^6 (60 dB) for the corresponding THz temporal intensity.

For comparison, in figure 2(*b*) the corresponding signal measured using the large-area GaAs emitter (1 kV cm^{-1} bias field) is shown, wihle results for the plasma emitters using SH-bias and external bias are depicted in figures 2(*c*) and (*d*), respectively.

The different detected THz waveforms from each emitter can be explained as follows. To begin with, we note that in principle the near-field temporal THz waveform directly after the large-area emitters is given by the temporal form of the surface current [7] (biased GaAs antenna) or the first derivative of the nonlinear polarization (optical rectification). In the far field (or in the focus of a focusing element) one detects an on-axis signal with a temporal form given by the first derivative of the near-field signal.

In contrast, for the plasma emitters (which are essentially THz point sources) one expects the following behaviour. In the far field of these point sources (e.g. at the position of the first collimating mirror) one expects a temporal signal given by the second derivative of the temporal development of the polarization in the plasma [36]. This temporal waveform is not changed by the collimating element and is thus maintained in the parallel THz beam path between the two mirrors. The last focusing element which creates the detector focus introduces a further derivation of the temporal signal [37]. In this way

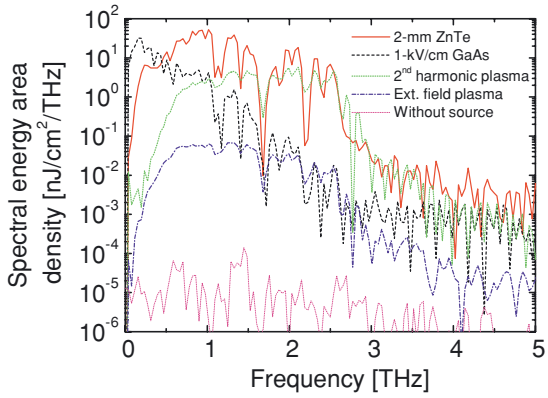

Figure 3. Power spectra of the various signals from figure 2.

one finally detects a signal with a temporal form given by the third derivative of the temporal development of the polarization inside the plasma volume.

Based on these assertions, the detected waveform of the large-area ZnTe emitter can be understood by considering the temporal form of the nonlinear polarization ($p_{\mathrm{NL}}(t)$) inside the electro-optic crystal, which is given by the temporal form of the optical intensity. If this is assumed to be Gaussian, then the detected signal is given by the second derivative of a Gaussian pulse, as illustrated in the two top left panels of figure 2.

For the detected waveform of the large-area GaAs emitter, we consider the temporal form of the surface current ($j_s(t)$). Due to the sudden change of the conductivity at the wafer surface induced by the incident optical pulse, the current changes abruptly from zero to an almost constant value which is dictated by THz-field self-screening [7]. This predicted stepwise behaviour results in a uni-polar detected THz pulse, as is illustrated in the two left panels in the second row of figure 2.

The temporal waveforms of the plasma sources can also be explained by considering their respective generation mechanisms. While the SH-bias method leads to a transient polarization inside the plasma which follows the temporal optical intensity, a stepwise behaviour is expected for the external-field method due to the ultrafast field-screening process. The resulting detected THz waveforms (third derivatives) from these models agree well with the experimentally-observed waveforms, as illustrated by the four bottom-left panels in figure 2.

In figure 3 the THz power spectra obtained by numerical Fourier transformation of the four signals in figures 2(*a*)–(*d*) are shown. In addition the dark-noise power spectrum (i.e. with the THz source blocked) is plotted. It is clear that the residual high-frequency noise floor when an actual THz signal is detected is much higher than the dark-noise level, due to fluctuations in the THz signal. We take this high-frequency noise level as representing the noise floor at lower THz frequencies as well. The magnitude of this additional noise contribution scales approximately with the total THz pulse energy, i.e. it is multiplicative in nature, and its source is chiefly from fluctuations in the optical pump pulse energy.

The power spectrum for the ZnTe emitter has a maximum near 1 THz with a clear low-frequency roll-off, and contains components which are 3.5 orders of magnitude above the noise floor for frequencies in the range 0.5–2.8 THz. The spectra for the plasma emitters are similar in shape to that of the large-area ZnTe emitter although with a reduction in the total pulse energy.

In contrast the power spectrum obtained from the large-area GaAs emitter is concentrated at lower THz frequencies, peaking at ∼100 GHz and decreasing by four orders of magnitude in the range up to 3 THz. This illustrates that for use in the range below 500 GHz the large-area GaAs emitter provides superior dynamic range, whilst for higher THz frequencies the large-area ZnTe and SH-bias plasma emitters are more suitable.

The pronounced oscillations in the time domain and the absorption lines in the frequency domain (e.g. at 1.1 THz and 1.6 THz) are due to water vapour absorption in the THz beam path. We note that the ZnTe emitter outperforms the GaAs emitter for the experimental parameters used here in terms of the detected maximum peak temporal amplitude, bandwidth and spectral power for frequencies >500 GHz.

7.3. Comparison of THz emitter performance

In order to compare the efficacy of each THz emitter in the amplifier-laser-based systems presented here, the question of how to formulate an appropriate definition of the figure-of-merit arises. Such a figure-of-merit could be based on simple direct quantities such as the maximum temporal THz electric field, the THz-pulse energy, the energy conversion efficiency or signal-to-noise properties. Of course, the relevant definition depends on the specific experimental situation, and also on the type of THz detector used (e.g. electro-optic detection versus bolometric THz power measurements).

A simplifying point for the different THz emitters presented here is that the ratio between the total THz-pulse energy and the square of the magnitude of the maximum THz temporal field are nearly the same for the large-area ZnTe and plasma-based emitters (due to the similarity in their spectra). Only the GaAs emitter exhibits a somewhat reduced peak THz field amplitude for a certain given THz-pulse energy relative to the other emitters. This is because the spectrum of this emitter is concentrated at relatively lower THz frequencies, as mentioned in the last section (see figure 3).

In order to provide an overview of the relative performance for each emitter, in figure 4 we show (*a*) measured peak THz electric field amplitudes (at the detector focus), (*b*) measured THz-pulse energies and (*c*) calculated energy conversion factors for the various emitter types.

It is important to point out that the highest THz field amplitudes reached so far (150 kV cm^{-1}, shown as a single star-shaped point in each panel of figure 4), have been obtained for a large-area GaAs emitter with pulsed bias fields [6]. As previously mentioned, this method has the disadvantage that it produces correspondingly larger background electrical noise, such that the higher signal level does not provide an increase in signal-to-noise. Using a large-area GaAs emitter with a static bias field of 1 kV cm^{-1}, THz field amplitudes of up to 10 kV cm^{-1} can be reached, as indicated by the data (square points) in figure 4. One characteristic feature of the GaAs emitter is its strong saturation for laser pulse energies exceeding 100 μJ. If one wants to make use of the high laser pulse energies available with low-repetition-rate table-top laser systems (e.g. energies in the 10–100 mJ range are available with 10 Hz laser systems), it would be necessary to employ emitters with a far larger area (or a mosaic of antenna elements) in order to achieve higher THz-pulse energies.

As can be seen in figure 4, at lower laser pulse energies the large-area ZnTe emitter exhibits significantly reduced performance compared to the biased GaAs emitter (for all quantities shown). However, the optical rectification process shows a far less pronounced saturation behaviour for higher laser pulse energies. We have previously experimentally determined this saturation behaviour for optical rectification in a 2-mm-thick ZnTe emitter crystal at higher intensities (using smaller pump beam diameters). These results allow us to extrapolate the expected THz signal and conversion efficiency for this emitter based on a phenomenological model employing the expression from standard cw SHG theory [22] ($\eta_{\mathrm{SHG}} \propto \tanh^2(\mathrm{const} \times \sqrt{I_{\mathrm{opt}}})$, see thin lines in figure 4). It is evident that for laser pulse energies above 1 mJ, the ZnTe emitter has the potential to easily outperform the state-of-the-art GaAs emitter.

We now address the measured THz field amplitudes of the various plasma sources discussed in this paper. The data in figure 4 for all the plasma sources show a threshold behaviour at ∼35 μJ because of the onset of plasma formation at this laser pulse energy with the optical beam parameters used (corresponding to an instantaneous optical field strength of $\sim 2 \times 10^{14}$ W cm^{-2} at the focus). Above this threshold, the THz field amplitudes reached with both the ponderomotive force and external-bias methods scale linearly with the laser pulse energy. This seemingly simple dependence is actually a result of the play-off between (i) the super-linear increase of the plasma volume with optical pulse energy [18] and (ii) phase mismatch and absorption effects occurring at larger plasma volumes.

Comparing the amplitudes of the THz fields generated at a laser pulse energy of 500 μJ, one finds that the values for the ponderomotive-force and external-field method fall below that of the statically-biased GaAs emitter by two and one orders of magnitude, respectively.

However, for this laser pulse energy the THz signal generated with the SH-bias plasma method is comparable with that of the GaAs emitter. At lower laser pulse energies (i.e. in the range below 100 μJ) the THz-generation efficiency of the SH-bias method converges towards that of the external-field method. However, at higher laser pulse energies the SH-bias method offers the advantage of a stronger (quadratic) increase of the THz signal with laser pulse energy. The reason for this higher-order dependence for the SH-bias emitter is described below.

Because of the onset of severe saturation for the standard GaAs emitter at higher optical pulse energies, it is interesting to examine the potential of the plasma sources for operation with very intense laser pulses (i.e. with energies of >10 mJ). Due to their respective THz generation mechanisms, for both the ponderomotive-force method and external-field method one expects that the THz signal will remain proportional to the

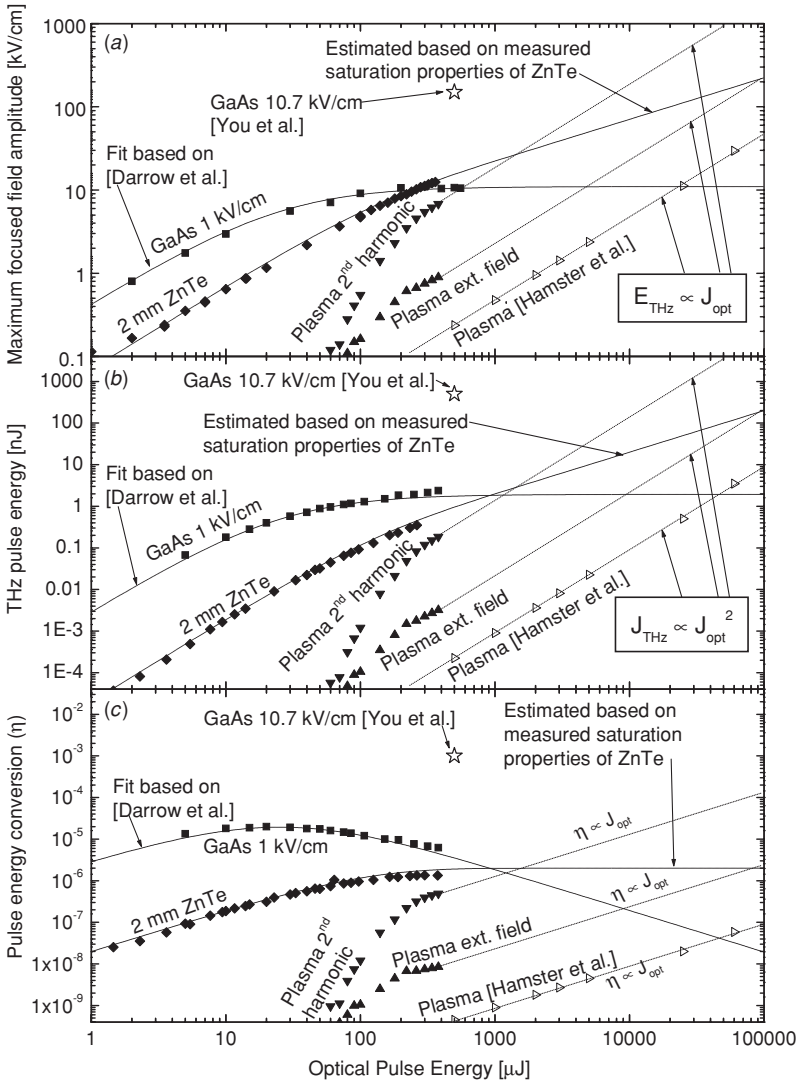

Figure 4. Comparison of (*a*) the focused peak electric field, (*b*) the THz-pulse energy and (*c*) the energy conversion efficacy.

plasma volume, with a gradual saturation behaviour introduced by phase mismatch and absorption effects. Indeed, the data of Hamster *et al* [11–13] exhibit a linear increase of the THz field amplitude obtained by the external-field method for laser pulse energies up to 10 mJ (see figure 4).

The analysis is somewhat more complex in the case of the SH-bias method because of the additional nonlinear SHG process involved. The maximum achievable SHG conversion efficiency for the experimental parameters described in this paper is ∼15%. This value results from phase-matching in the BBO crystal and the maximum optical fluence before damaging the crystal. For our experimental set-up, this limit is reached in approaching the maximum available pulse energy of 500 μJ. If the laser pulse energy were to be further increased, an increase in the emitted THz amplitude would only result from the increase of the plasma volume, provided that the SHG conversion efficiency remained clamped at the maximum value of 15% (which would require one to correspondingly increase the illuminated area of the BBO crystal). Hence in this optical pulse energy regime, one can expect only a linear increase of the THz signal amplitude as for the other plasma emitters. Based on these assumptions, the SH-biased plasma emitter could still produce focused THz-field amplitudes of the order of ∼150 kV cm^{-1} for optical pump pulse energies of ∼10 mJ. This is equivalent to the maximum reported level achieved with pulsed-bias GaAs emitters, although with the advantage of a broader THz spectrum and a greatly reduced background noise level.

Motivated by these predictions, we are currently performing plasma-emitter THz experiments at the front end of the PHELIX laser system at GSI (Gesellschaft für Schwerionenforschung, Darmstadt, Germany) in order to explore this laser pulse regime experimentally.

8. Summary

In summary, we have reviewed a range of THz-pulse generation mechanisms suitable for use with table-top amplifier-laser-based THz systems. From a comparison of the THz signals from each emitter, we conclude that the ZnTe emitter shows the best overall performance in the pulse energy range which can be achieved with 1 kHz amplifier

laser systems. We also predict that for higher laser pulse energies (i.e. above ∼1 mJ) the emitter based on a second-harmonic-biased plasma shows the potential to outperform the conventional large-area THz emitters, which suffer from saturation effects in this pulse energy regime.

Acknowledgment

This work was funded in part by GSI (Gesellschaft fr Schwerionenforschung), Darmstadt, Germany, under contract no. OF-ROS.

References

[1] Auston D H, Cheung K P and Smith P R 1984 *Appl. Phys. Lett.* **45** 284
[2] Hu B B, Zhang X-C, Auston D H and Smith P R 1990 *Appl. Phys. Lett.* **56** 506
[3] Han P Y and Zhang X-C 1998 *Appl. Phys. Lett.* **73** 3049
[4] Nahata A, Welling S A and Heinz T F 1996 *Appl. Phys. Lett.* **69** 2321
[5] Zhang X-C, Darrow J T, Hu B B, Auston D H, Schmidt M T, Tharn P and Yang E S 1990 *Appl. Phys. Lett.* **56** 2228
[6] You D, Jones R R and Bucksbaum P H 1993 *Opt. Lett.* **18** 290
[7] Darrow J T, Zhang X-C and Auston D H 1992 *IEEE J. Quantum Electron.* **28** 1607
[8] Carrig T J, Rodriguez G, Clement T S and Taylor A J 1995 *Appl. Phys. Lett.* **66** 10
[9] Carrig T J, Rodriguez G, Clement T S, Taylor A J and Stewart K R 1995 *Appl. Phys. Lett.* **66** 121
[10] Löffler T, Hahn T, Thomson M, Jacob F and Roskos H G 2005 *Opt. Express* in preparation
[11] Hamster H, Sullivan A, Gordon S, White W and Falcone R W 1993 *Phys. Rev. Lett.* **71** 2715
[12] Hamster H 1993 *PhD Thesis* University of Berkeley
[13] Hamster H, Sullivan A, Gordon S and Falcone R W 1994 *Phys. Rev.* E **49** 671
[14] Cook D J and Hochstrasser R M 2000 *Opt. Lett.* **25** 1210
[15] Cook D J and Hochstrasser R M 2000 *Ultrafast Phenomena XII (Springer Series of Chemical Physics)* vol 66 p 197
[16] Löffler T, Jacob F and Roskos H G 2000 *Appl. Phys. Lett.* **77** 453
[17] Löffler T and Roskos H G 2002 *J. Appl. Phys.* **91** 2611
[18] Kreß M, Löffler T, Eden S, Thomson M and Roskos H G 2004 *Opt. Lett.* **29** 1120
[19] Jones R R, You D and Bucksbaum P H 1993 *Phys. Rev. Lett.* **70** 1236
[20] Segschneider G, Jacob F, Löffler T, Roskos H G, Tautz S, Kiesel P and Döhler G 2002 *Phys. Rev.* B **65** 125205
[21] Wu Q, Hewitt T D and Zhang X-C 1996 *Appl. Phys. Lett.* **69** 1026
[22] Yariv A 1989 *Quantum Electronics* vol 3 (New York: Wiley)
[23] Zhang X-C, Hu B B, Darrow J T and Auston D H 1990 *Appl. Phys. Lett.* **56** 1011
[24] Benicewicz P K, Roberts J P and Taylor A J 1994 *J. Opt. Soc. Am.* B **11** 2533
[25] Budiarto E, Pu N-W, Jeong S and Bokor J 1998 *Opt. Lett.* **23** 213
[26] Rodriguez G and Taylor A J 1996 *Opt. Lett.* **21** 1046
[27] Hasegawa N *et al* 2003 *CLEO 2003*
[28] Löffler T, Siebert K, Czasch S, Bauer T and Roskos H G 2002 *Phys. Med. Biol.* **47** 3847
[29] Löffler T, Bauer T, Siebert K, Roskos H G, Fitzgerald A and Czasch S 2001 *Opt. Express* **9** 616
[30] Hasegawa N, Löffler T, Thomson M and Roskos H G 2003 *Appl. Phys. Lett.* **83** 3996
[31] Geissler M and Brabec T 2001 *28th EPS Conference on Controlled Fusion and Plasma Physics (Funchal) Eur. Conf. Abstr.* **25** A 2017
[32] Löffler T, Kreß M, Thomson M and Roskos H G 2005 *Acta Phys. Pol.* A **107** 99
[33] Löffler T 2003 *PhD Thesis* JWG University Frankfurt Germany, http://deposit.ddb.de/cgi-bin/dokserv?idn=96998541x
[34] Haberland H, Bonitz M and Kremp H 2001 *Phys. Rev.* E **64** 026405
[35] Löffler T *et al* 2005 *Phys. Rev. Lett.* in preparation
[36] Jackson J D 1975 *Classical Electrodynamics* vol 2 (Reading, MA: Addison-Wesley)
[37] Gürtler A, Winnewisser C, Helm H and Jepsen P U 2000 *J. Opt. Soc. Am.* A **17** 74